

# THE MEASUREMENT OF DIFFUSION USING PULSED NMR

I.J. Lowe

Department of Physics and Astronomy  
University of Pittsburgh  
Pittsburgh, PA, U.S.A.

## I. INTRODUCTION

Pulsed NMR is the most convenient and powerful technique for measuring diffusion, when it is applicable. Hahn (1) in a seminal paper laid the foundations of the technique. He showed that for a nuclear spin system that obeyed the Bloch equations (taking small liberties with exact details), a  $90^\circ - \tau - 180^\circ$  RF pulse sequence produced a free induction decay (FID) and an echo, as pictured in Figure 1. The FID had an initial amplitude  $A_0$  and a shape  $f(t)$  that was the Fourier transform of the frequency distribution function  $g(\Delta\omega)$  that described the magnetic field distribution over the sample [ $f(0) = 1$ ]. The echo had a shape  $A_e(2\tau)f(t - 2\tau)$ , and peaked at  $t = 2\tau$  with a value

$$A_e(2\tau) = A_0 \exp [2\tau / T_2 - \frac{2}{3} (\gamma G_0)^2 D \tau^3] \quad (1)$$

where

$\gamma$  = magnetogyric ratio of the observed spins

$T_2$  = transverse relaxation time of observed spins

$D$  = bulk diffusion coefficient of the observed spins

$\vec{G}_0$  = static magnetic field gradient.

The attenuation of the echo due to  $T_2$  can be separated from echo attenuation due to diffusion by the  $\tau$  and  $\tau^3$  dependence of the two mechanisms. The  $T_2$  effects can also be corrected for by first measuring the echo attenuation in a relatively homogeneous magnetic field and then repeating the measurement in a magnetic field with a known large gradient.

Carr and Purcell (2)—CP—extended the technique by showing that the effects of diffusion on the attenuation of an echo can be reduced by using many  $180^\circ$  RF pulses. The CP sequence is pictured in Figure 2. Following a  $90^\circ$  pulse at  $t = 0$ ,  $180^\circ$  pulses are applied at time  $\tau, 3\tau, 5\tau, \dots, (2n - 1)\tau$ , with echoes occurring at times  $2\tau, 4\tau, 6\tau, \dots, 2n\tau$ . The peak amplitude of the  $n$ th echo, occurring at time  $t$  and  $2n\tau$ , is given by

$$A_e(2n\tau) = A_0 \exp [-2n\tau / T_2 - \frac{2}{3} (\gamma G_0)^2 D n\tau^3] \quad (2)$$

$$= A_0 \exp [(-t / T_2) - (\gamma G_0)^2 D t^3 / 12n^2]$$

Eq. 2 demonstrates that the effects of diffusion on the echo occurring at time  $t$  can be reduced by a factor  $n^2$ , where  $n$  is the number of  $180^\circ$  pulses applied between times 0 and  $t$ .

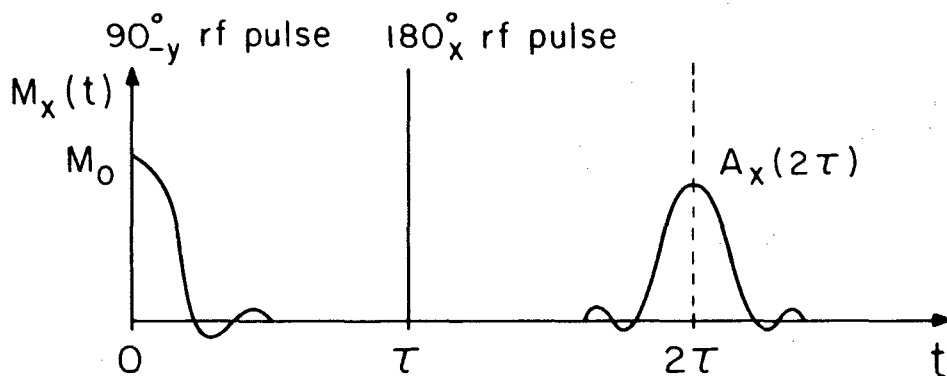


Figure 1:  $90_y - \tau - 180_x$  RF pulse sequence with spin system response of a free induction decay and echo.

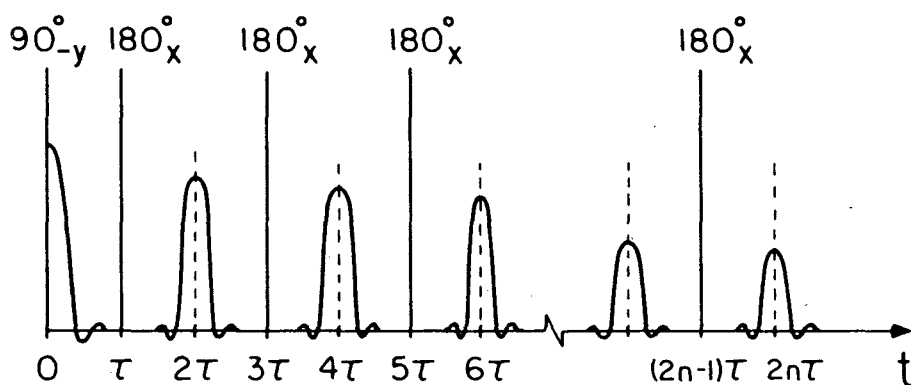


Figure 2. Carr-Purcell RF pulse sequence with spin system response of a free induction decay and echoes.

Stejskal and Tanner (3)—ST—added one more variable to the techniques of studying diffusion by making the gradient that appears in the Hahn  $90_y - 180_x$  pulse sequence time dependent. The RF excitation pulses, the gradient pulses, and the resultant spin response are pictured in Figure 3. The response of the echo at time  $2\tau$  is given by

$$A(2\tau) = A_0 \exp \left[ -2\tau / T_2 - \gamma^2 D \left\{ \frac{2}{3} G_0^2 \tau^3 + \delta^2 G_A^2 (\Delta - \delta / 3) - \delta \vec{G}_0 \cdot \vec{G}_A [(t_1^2 + t_2) + \delta(t_1 + t_2) + \frac{2}{3} \delta^2 - 2\tau^2] \right\} \right] \quad (3)$$

where

$\vec{G}_0$  = the time independent gradient (usually a background gradient)

$\vec{G}_A$  = the pulsed magnetic field gradient

$t_1$  = time between  $90_y$  RF pulse and field gradient pulse

$\delta$  = length of time field gradient pulse is applied

$\Delta$  = time between leading edges of the first and second field gradient pulses

$$t_2 \equiv 2\tau - (\delta + \Delta + t_1).$$

When  $G_A^2 \delta^2 \Delta \gg G_0^2 \tau^3$ , Eq. (3) simplifies to

$$A(2\tau) = A_0 \exp \left[ (-2\tau / T_2) - \gamma^2 G_A^2 D \delta^2 (\Delta - \delta / 3) \right] \quad (4)$$

While the ST technique is more complicated experimentally, it has the advantage that a large gradient  $G_A$  can be applied to the spin system without producing a very narrow, and difficult to measure, echo. It also has the disadvantage of having a  $\vec{G}_0 \cdot \vec{G}_A$  cross term that can sometimes prove to be troublesome.

To get a heuristic understanding of why a  $90_y - 180_x$  pulse sequence produces an echo in an inhomogeneous magnetic field, and why the effects of diffusion attenuate the echo, one may use the analogy (due to Hahn) of a group of runners jogging around a track. Due to track conditions (such as muddiness), lane 3 is the fastest, lane 2 is next to the fastest, and lane 1 is the slowest. These different

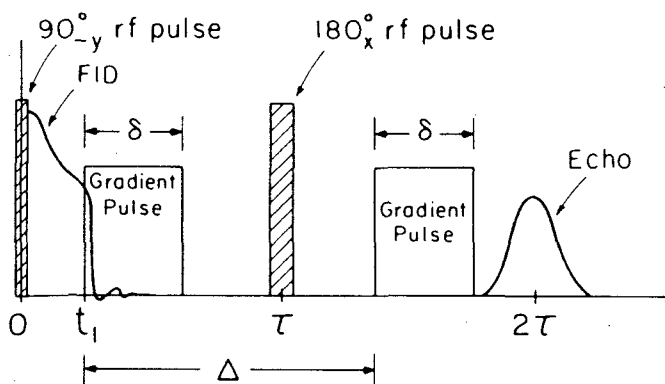


Figure 3. Stejskal-Tanner pulsed gradient-spin echo sequence.

lanes correspond to different parts of the sample in an inhomogeneous magnetic field. The Larmor speed of the spins in one part of the sample are different than in another part of the sample.

At time  $t=0$ , the three runners start together at the starting line, running clockwise as shown in Figure 4 ( $90^\circ$  RF pulse). Assume first that each runner stays in his original starting lane. At time  $\tau$ , each will have run a different distance, with the runner in track 3 having run the farthest. This corresponds to the dephasing of the spins and the decay of the free induction signal. At time  $\tau$ , a signal is given to the runners to reverse their direction and run counterclockwise (equivalent to the  $180^\circ$  RF pulse). If the runners remain in their own lane and maintain their original speed, they will arrive back together at the starting line at time  $2\tau$ . This corresponds to the rephasing of the spins and the production of an echo. Because the runners arrive back together, the equivalent echo height is the same as the initial value of the FID, and independent of  $\tau$ . If the runners are allowed to randomly change lanes during time  $0$  to  $\tau$  and  $\tau$  to  $2\tau$  (corresponding to the particles diffusing from one part of the sample to another), the runners' speeds also vary in a random way. Then, they will not all arrive back together at the starting line at time  $2\tau$  since  $\int_0^\tau v(t)dt$  may be different from  $\int_\tau^{2\tau} v(t)dt$ . This corresponds to the echo being attenuated because not all the spins rephase at the starting line at time  $2\tau$ . The bigger  $\tau$  is, the greater the dephasing and the smaller the echo. If the experiment is repeated a number of times, sometimes runner 1 will arrive first, sometimes runner 2 and sometimes runner 3.

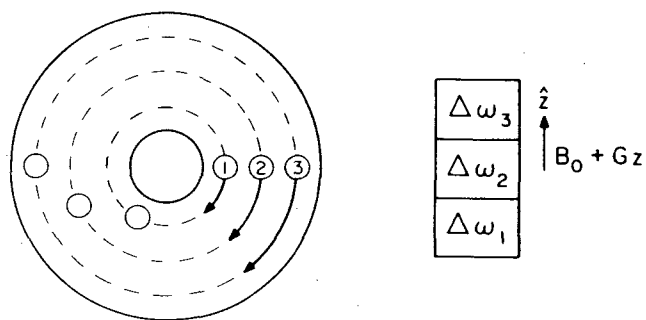


Figure 4. Joggers running around a muddy track. Lane 3 conditions are best, so any runner in lane 3 is able to run fastest. This corresponds to region 3 where the applied magnetic field is greatest so that spins have the fastest Larmor speed.

## II. THEORY

### A. Derivation of Diffusion Term in Bloch Equation

The attenuation of echoes due to diffusional motion of particles can be calculated using the Bloch equation. Following Torrey (4),  $\vec{M}(\vec{r}, t)$  is defined as the magnetization vector per unit volume at position  $r$  in the sample at time  $t$ . Assuming that the various sources of time dependence of  $\vec{M}(\vec{r}, t)$  are independent of one another, we write (suppressing the position dependence of  $M$  for the moment).

$$d\vec{M}/dt = (\partial \vec{M}/\partial t)_{mag. field} + (\partial \vec{M}/\partial t)_{relaxation} + (\partial \vec{M}/\partial t)_{diffusion} \quad (5)$$

$$(d\vec{M}/dt)_{mag. field} = \gamma \vec{M} \times \vec{B} \quad (6)$$

$$(\partial \vec{M}/\partial t)_{relaxation} = -[(M_x \hat{x} + M_y \hat{y})/T_2] + [(M_0 - M_z)\hat{z}/T_1] \quad (7)$$

$\gamma$  = magnetogyric ratio of observed nuclei,

$\vec{B}(\vec{r}, t)$  = the applied magnetic field at position  $\vec{r}$  in the sample at time  $t$ ,

$T_1, T_2$  = nuclear spin-lattice and spin-spin relaxation times respectively

$M_0$  = Equilibrium magnetization as given by the Curie law.

To find the form of the third term in Eq. 5, let us examine the equation of motion of a set of particles that

can be labeled in some way, and for which there is a non-equilibrium density distribution  $\rho(\vec{r}, t)$ . The time and spatial dependence of  $\rho(\vec{r}, t)$  are connected by the diffusion equation

$$\partial \rho / \partial t = D \nabla^2 \rho \quad (8)$$

and are almost independent of the label on the particle. For the sake of simplicity,  $D$ , the bulk diffusion rate, will be assumed to be isotropic and independent of position in the sample. Probably the most innocuous label that a particle can carry is the direction of its angular momentum vector  $\vec{l}$ . It will be assumed that the angular momenta are classical (obey the vector model) and have a magnetic moment  $\vec{\mu} = \gamma \vec{l}$ . Let  $n(\theta, \phi, \vec{r}, t)$  be the number of particles per unit volume at position  $\vec{r}$  in the sample at time  $t$ , whose magnetic moment  $\vec{\mu}$  points in the direction described by the spherical angles  $\theta, \phi$ .

Then

$$\vec{M}(\vec{r}, t) = \int_{4\pi} \int \vec{\mu} n(\theta, \phi, \vec{r}, t) d\Omega \quad (9)$$

$n$  satisfies Eq. 8, so that one can write

$$(\partial n / \partial t)_{diffusion} = D \nabla^2 n \quad (10)$$

Multiplying both sides of Eq. 10 by  $\vec{\mu}$  and integrating over  $\theta$  and  $\phi$

yields

$$\int_{4\pi} \int \vec{\mu} (\partial n) / (\partial t) d\Omega_{diffusion} = \int_{4\pi} \int \vec{\mu} D \nabla^2 n d\Omega \quad (11)$$

The order of integration over  $\theta$  and  $\phi$  is interchangeable with differentiation with respect to time and with respect to spatial position, so that:

$$\partial / \partial t \int_{4\pi} \int \vec{\mu} n d\Omega = D \nabla^2 \int_{4\pi} \int \vec{\mu} n d\Omega \quad (12)$$

Using Eq. 9, we get

$$[(\partial / \partial t) \vec{M}(\vec{r}, t)]_{diffusion} = D \nabla^2 \vec{M}(\vec{r}, t) \quad (13)$$

Combining Eqs. 5, 6, and 7 yields the modified Bloch equations

$$dM_x / dt = \gamma (\vec{M} \times \vec{B})_x - M_x / T_2 + D \nabla^2 M_x \quad (14)$$

$$dM_y / dt = \gamma (\vec{M} \times \vec{B})_y - M_y / T_2 + D \nabla^2 M_y \quad (15)$$

$$dM_z / dt = \gamma (\vec{M} \times \vec{B})_z + (M_0 - M_z) / T_1 + D \nabla^2 M_z \quad (16)$$

## B. Outline of Solution of Bloch Equation

It will now be assumed that

$$|\vec{b}(\vec{r}, t)| \ll B_0 \quad (17)$$

so that  $T_1$ ,  $T_2$ , and  $M_0$  can be assumed to be independent of position. As shown in the Appendix, since  $|\vec{b}| \ll B_0$ , only the  $z$  component of  $\vec{b}$  is important so that  $b_x$  and  $b_y$  can be dropped.

For a  $90^\circ$  RF excitation pulse followed by a number of  $180^\circ$  RF excitation pulses, and static and time-dependent field gradients, the general solution for the peak echo heights is relatively easy to find. To do so, we consider the motion of an isochromat from times  $T$  to  $T + \tau$ , with a  $180^\circ$  RF pulse being applied at time  $T + \tau$ . It will be assumed that at time  $T$ , the isochromat makes an angle  $\phi(T)$  with respect to the  $\hat{x}'$  axis in the rotating reference frame rotating at  $\omega_0 = \gamma B_0$ . The isochromat will accumulate phase  $\Delta\phi = \gamma b_z \tau$  during time  $\tau$ .

After the  $180^\circ$  pulse at  $T + \tau$ , the phase of the isochromat relative to  $\hat{x}'$  is  $-\phi(T) - b_z \tau$ . For times  $t > T + \tau$ , this phase could have been produced by moving the  $180^\circ$  RF pulse back to time  $T$ , and having the spins evolve in the field  $-b_z$  for a time  $\tau$ . Thus, for the purposes of computing the phase of an isochromat at times  $t > T + \tau$ , the two sequences are equivalent. If another  $180^\circ$  pulse had occurred at time  $T$ , the two pulses would add up to  $360^\circ = 0^\circ$ , that is no pulse at all. For the purposes of working out the motion of an isochromat, the  $180^\circ$  RF pulses can be eliminated and the field  $b_z$  flipped back and forth. This can be viewed as a transformation into what might be called the flip-flop frame (see Figure 5).

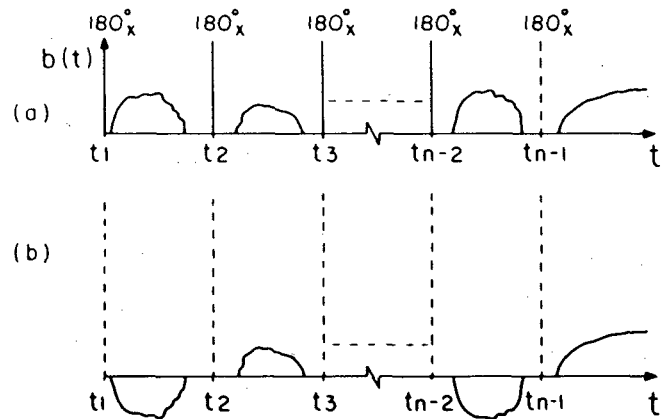


Figure 5. (a) Time-dependent gradient pulses interspersed among  $180^\circ$  RF pulses. (b) Elimination of the  $180^\circ$  RF pulses, with the transformation of the gradients into the flip-flop frame.

As derived in the appendix, when  $b_z(\vec{r}, t)$  is linearly dependent upon position (constant magnetic field gradient), that is

$$b_z(\vec{r}, t) = \vec{G}(t) \cdot \vec{r} = G_x x + G_y y + G_z z \quad (18)$$

a general solution for the peak echo heights can be found. This general solution is

$$A(t_n) = A_0(t_n) \exp \left[ -\gamma^2 D \sum_{j=1,2,3} \int_0^{t_n} K_j^2(t') dt' \right] \quad (19)$$

where

$$A_0(t_n) = A_0 \exp[-t_n/T_2] \quad (20)$$

$$K_j(t') = \int_0^{t'} G_j(t'') dt'' \quad j=1,2,3 \quad (21)$$

and  $A_0$  is a constant such as  $M_0$  (as when the RF excitation pulse at time 0 produces a  $90^\circ$  rotation). The  $n$ th echo peak occurs at time  $t_n$  such that

$$\int_0^{t_n} G_j(t'') dt'' = 0 \quad (22)$$

It is typically assumed that one of the  $G_j$ 's dominates, so that the other two can be set equal to zero. Thus, it will be assumed that  $G_x = G_y = 0$ , and  $G_z = G_0$ .

### C. Applications to Various Pulse Sequences

The calculation of the effects of diffusion using Eqs. 19-21 is quite easy, even for complicated pulse sequences.

#### 1. $90^\circ - \tau - 180^\circ - \tau$ - Echo Sequence with Static Gradient $G$

In the flip-flop frame, the gradient  $G(t'')$  appears to have the values (see Figure 1)

$$G(t'') = -G_0 \quad \text{for } 0 \leq t'' \leq \tau$$

$$G(t'') = G_0 \quad \text{for } \tau \leq t''$$

Thus,

$$\int_0^{t'} G(t'') dt'' = -G_0 t' \quad \text{for } 0 \leq t' \leq \tau$$

$$\int_0^{t'} G(t'') dt'' = G_0(t' - 2\tau) \quad \text{for } \tau \leq t'$$

The echo occurs at  $2\tau$  where  $\int_0^{2\tau} G_0(t'') dt'' = 0$ . Inserting the above into Eq. 19 yields

$$\ln A(2\tau)/A_0(2\tau) = -\gamma^2 D \left\{ \int_0^\tau [-G_0(t')]^2 dt' + \int_\tau^{2\tau} [G_0(t' - 2\tau)]^2 dt' \right\} = -2\gamma^2 G_0^2 \tau^3 / 3 \quad (23)$$

#### 2. Carr Purcell Sequence — Static Gradient $G_0$

Referring to Figure 2, it can be seen that for the Carr-Purcell sequence of RF pulses, the gradient in the flip-flop frame appears to have the time dependence depicted in Figure 6. Thus  $K(t')$  has a sawtooth shape, also depicted in Figure 6 and

$$\begin{aligned} \ln[A(2n\tau)/A_0(2n\tau)] &= -\gamma^2 D_0 \int_0^{2n\tau} K^2(t') dt' = \\ &= -\gamma^2 D(2n) \int_0^\tau G_0^2 t'^2 dt' = -2n(\gamma G_0)^2 D\tau^3 / 3 \end{aligned} \quad (24)$$

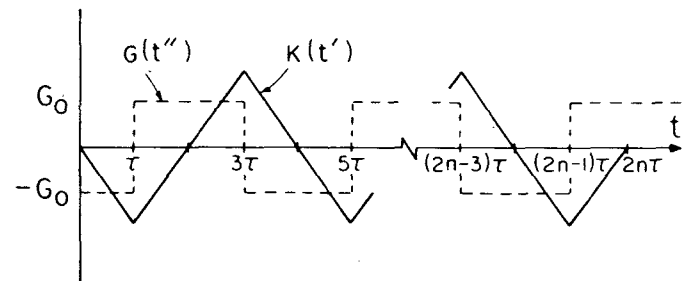


Figure 6. A view from the flip-flop frame of the static gradient  $G_0$  for a Carr-Purcell sequence (dotted lines). The solid lines are  $K(t') = \int_0^{t'} G(t'') dt''$ .  $K(t')$  passes through zero at  $2\tau, 4\tau, \dots, 2n\tau$  where echoes occur.

#### 3. Alternating Pulse Field Gradient Technique

The alternating pulse field gradient technique (APFG) (5) combines a Carr-Purcell string to RF pulses with a string of pulsed field gradients that alternate in sign. The APFG sequence in its simplest form of five  $180^\circ$  RF pulses is pictured in Figure 7;  $G_A$  is the amplitude of the pulsed field gradient and  $G_0$  is the background gradient. The APFG sequence as viewed in the flip-flop frame is pictured in Figure 8. Using the flip-flop frame picture and Eqs. 19-21, it is relatively easy to obtain the result

$$\begin{aligned} \ln[A(10\tau)/A_0(10\tau)] &= \\ &= -2\gamma^2 D\tau^3(5G_0^2 + 64G_A^2)/3 \end{aligned} \quad (25)$$

From Figure 8, the results in Eq. 25 are easy to interpret. The contribution of  $5G_0^2$  is that due to a Carr-Purcell string of five RF pulses acting on the field gradient  $G_0$ . The second term  $64G_A^2$  is the result of a  $90^\circ - 4\tau - 180^\circ - 4\tau$  pulse sequence acting on a field gradient of  $G_A$ , as pictured in Figure 8. Most important of all, it is observed that there is no cross term between  $\vec{G}_0$  and  $\vec{G}_A$ .

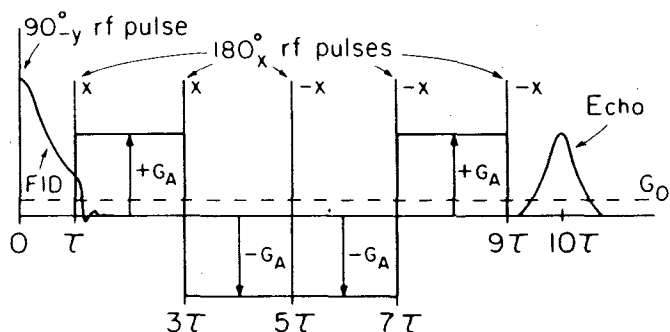


**Figure 7.** The APFG sequence. It is used for measuring diffusion in the presence of background magnetic field gradients. The dotted line represents the background gradient  $G_0$ , and the solid line represents the pulsed field gradient  $G_A$ .

The calculations for the APFG sequence can be further generalized to the case of  $n$   $180^\circ$  RF pulses and  $n-1$  gradient. The leading and trailing edges of the gradient pulses are assumed to be separated from the neighboring RF pulses by times  $\delta_1$  and  $\delta_2$ , respectively. The result is

$$\ln[A(2n\tau)/A_0(2n\tau)] = -\frac{2}{3}\gamma^2 D [nG_0^2\tau^3 + \quad (26)$$

$$(n-1)^3 G_A^2 (\tau - \frac{1}{2}(\delta_1 + \delta_2))^2 (\tau + (\delta_1 + \delta_2)/(n-1)^2)]$$

If we ignore  $\delta_1$  and  $\delta_2$ , Eq. 26 shows that the ratio of the affects of the background gradient  $G_0$  to the applied gradient  $G_A$  decreases as  $n/(n-1)^3$ . Practical considerations, such as the rise and fall times of gradient pulses, shapes of RF pulses, and  $T_2$  put a limit on the value of  $n$ .

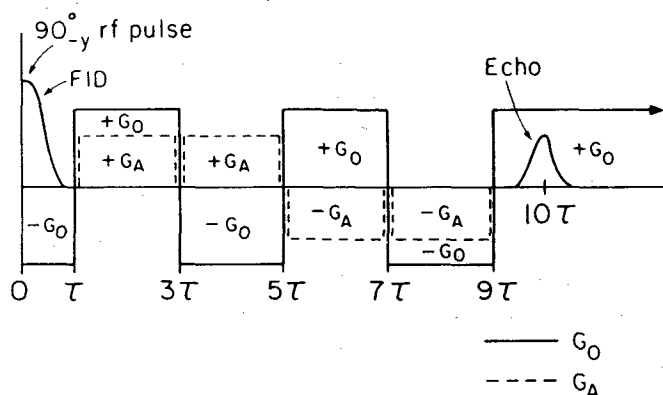


**Figure 8.** A view from the flip-flop frame of the APFG sequence.

### III. TEST OF THE APFG SEQUENCE

It has been experimentally verified that the APFG technique can eliminate the  $\vec{G}_0 \cdot \vec{G}_A$  cross term and permit the measurement of  $D$  in the presence of large, static, background gradients (5).  $D$  was measured for  $H_2O$  at room temperature with  $G_0 = 0$  and then with  $G_0 = 160$  G/cm.  $G_0$  was generated by placing a pair of iron wedges against the pole caps of an electromagnet, and  $G_A$  was generated by pulsing a quadrupole coil placed around the sample.

Shown in Figure 9 is a plot of the log(echo attenuation) vs  $G_A^2$ , obtained from an APFG sequence in which the echo occurs at  $t=10\tau$ , and  $\tau = 300 \mu s$ ,  $\delta_1 = \delta_2 = 10 \mu s$ , and  $G_0 = 160$  G/cm. The value of  $D$  of  $H_2O$  (tap water, lightly doped with  $CuSO_4$ ) at  $23.9^\circ C$  was determined from the slope of the straight line in Figure 9 to be  $(2.29 \pm 0.1) \times 10^{-5}$   $cm^2/sec$  by using the following relation for the APFG sequence

$$D = 3 [(-d \ln A(10\tau))/d(G_A^2)] / 128\delta^2 X, \quad (27)$$

$$X = [\tau - \frac{1}{2}(\delta_1 + \delta_2)]^2 [\tau + (\delta_1 + \delta_2)/16]$$

This value for  $D$  of  $H_2O$  agrees well with literature values (6) and, more importantly, agrees, within experimental error, with the value of  $D$  obtained from the same APFG sequence with  $G_0 \sim 0$ .

One can use the results of the APFG measurements to calculate the value of  $G_0$ . Setting  $G_A = 0$  in Eq. 26 yields

$$G_0 = \frac{\{[\ln A_0(10\tau) - \ln A(10\tau)]_{G_A=0}\}^{1/2}}{10\gamma^2 D \tau^3 / 3} \quad (28)$$

The term  $\ln A(10\tau)_{G_A=0}$  is just the intercept at  $G_A = 0$  of the plot of  $\ln A(10\tau)$  vs  $G_A^2$ , as shown in Figure 9, while the diffusion constant  $D$  is determined from the slope of that curve using Eq. 27. The term  $A_0(10\tau)$ , the predicted echo height at time  $10\tau$  that excludes the effects of diffusion, can be found by using a Carr-Purcell string of pulses that are close enough together to effectively quench the effects of diffusion in the background gradient  $G_0$ . The value of  $G_0$  calculated in this manner from the intercept in Figure 9, using the measured values of  $D$  and  $A_0(10\tau)$ , is 152 G/cm, which is, within the experimental error, the value of  $G_0$  determined from the echo shape.

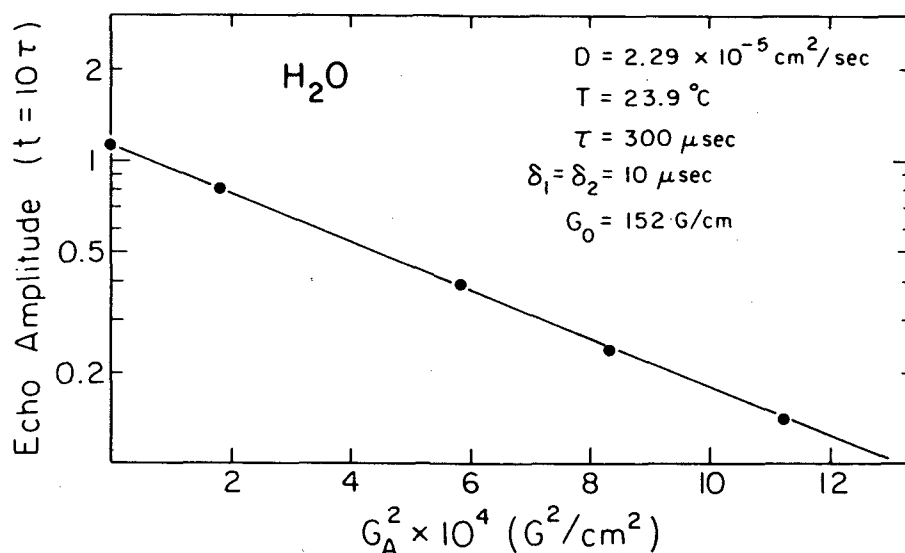


**Figure 9.** The measurement of  $D$  in  $\text{H}_2\text{O}$  in the presence of a 160-G/cm background gradient using the APFG technique. The quantity  $D$  was evaluated from the slope of the line obtained from a plot of  $\ln(\text{echo amplitude})$  vs  $G_A^2$ , using Eq. 27. The same value for  $D$  of  $\text{H}_2\text{O}$  was obtained using the APFG technique with  $G_0 = 0$ .

#### IV. THE MEASUREMENT OF DIFFUSION IN FINE POWDERS

Pulsed NMR is widely used to measure diffusion in solids, liquids, powders, and biological tissues. For liquids and solids, a constant-gradient technique can be used, but for powders, a pulsed-field-gradient technique is often necessary. In powdered samples, a distribution of internal magnetic fields is produced by the magnetization of each individual particle due to the volume magnetic susceptibility of the material being studied. The magnetic field inside each particle shape and the packing arrangement of neighboring particles. This distribution of magnetic fields within each particle can be as large as a few gauss in materials with a large bulk magnetic susceptibility. Since this variation in magnetic field is over the dimensions of a single particle, the background gradients can be expressed as (7)

$$\langle G_0 \rangle \approx \langle \Delta B \rangle / \langle d \rangle \quad (29)$$

where  $\langle \Delta B \rangle$  is the average width of the magnetic field distribution within the particles of the powdered sample,  $\langle d \rangle$  is the average particle size, and  $\langle G_0 \rangle$  is an effective  $G_0$ . Thus, if  $\Delta B$  for a particular powdered sample under investigation is 1 G and the average particle size is 1  $\mu\text{m}$ , then  $G_0$  may be as large as 10 kG/cm. Furthermore, for most powdered samples, there is a distribution of particle sizes and shapes and  $G_0$  is not uniform throughout the sample. Additional contributions to  $G_0$  can come from fer-

romagnetic inclusions in and on the surface of the fine powder.

Under such circumstances, the APFG sequence seems to be one of the better ways to measure diffusion in these fine powders since, by making the number of pulses  $n$  big enough, the effects of  $G_A$  can be made to dominate those by  $G_0$ .

#### Lanthanum Nickel Hydride

Lanthanum Nickel ( $\text{LaNi}_5$ ) is a rare earth intermetallic compound that has considerable technological and scientific interest. It is a Pauli paramagnet, very brittle, and a reasonably good electrical conductor, and it absorbs large amounts of hydrogen at room temperature and several bars of pressure.  $\text{LaNi}_5\text{H}_x$  has two phases: the  $\alpha$  phase where  $x < 0.6$ , and the  $\beta$  phase where  $6 < x$ . The lattice volume increases by 0.25 in the  $\alpha \rightarrow \beta$  transition, and the metal spontaneously crumbles into a fine powder during this transition. There is a distribution of local magnetic fields in this powder due to all the reasons listed earlier. The diffusion rate of hydrogen in this material has been measured using the APFG sequence (8).

Pulsed field gradients of up to 1200 G/cm were used.  $D$  was found to follow Arrhenius behavior. Thus

$$D = D_0 \exp(-E_a / RT) \quad (30)$$

with  $D_0 = 0.14 (\pm 0.03) \text{ cm}^2/\text{sec}$

$$E_a = 40 (\pm 4) \text{ kJ/g-atom-H}$$

The smallest diffusion constant that was measured was  $6 \times 10^{-8}$  cm<sup>2</sup>/sec, and the measured  $\langle G_0 \rangle$  was  $6(\pm 1)$  kG/cm.

## V. APPENDIX

The Bloch equations, Eqs. 14-16 are solved following Torrey (4) and Lowe (5). We start by defining  $M_x = M_x + iM_y$ ,  $M_z = M_z - iM_y$ ,  $b_x = b_x + ib_y$ ,  $b_z = b_x - ib_y$ , and  $\omega_0 = \gamma B_0$ . Eqs. 14-16 can then be rewritten as

$$dM_x/dt = (-i\omega_0 - 1/T_2 - i\gamma b_z + D\nabla^2)M_x + i\gamma b_x M_z \quad (A1)$$

$$dM_z/dt = (i\omega_0 - 1/T_2 + i\gamma b_z + D\nabla^2)M_z - i\gamma b_x M_x \quad (A2)$$

$$dM_y/dt = \frac{1}{2}\gamma i(M_x b_z - M_z b_x) + (M_0 - M_z)/T_1 + D\nabla^2 M_y \quad (A3)$$

From the definition above, it follows that  $M = M_x^*$ . Eqs. A1 and A2 are consistent with this definition.

From the arguments presented in Section IIB, the behavior of  $M_x$  and  $M_z$  in experiments where 180° RF pulses are applied to the sample can be found by solving Eq. A1 with  $\omega_0$ ,  $b_x$ , and  $M_z$  assuming the transformations produced by the 180° pulses listed in Eq. A4

$$\begin{aligned} b_x &\rightarrow -b_x \\ b_z &\rightarrow b_z \\ b_y &\rightarrow b_y \end{aligned} \quad (A4)$$

$$B_0 \rightarrow -B_0, \omega_0 \rightarrow -\omega_0, M_0 \rightarrow -M_0$$

We now define  $\vec{M}_x(\vec{r}, t)$  as

$$M_x(\vec{r}, t) = \exp[-t/T_2 - i \int_0^t \omega_0(t') dt'] \cdot m_x(\vec{r}, t) \quad (A5)$$

and substitute it into Eq. A1. The result is

$$\begin{aligned} m_x &= (-i\gamma b_x + D\nabla^2)m_x + \\ & i\gamma b_x \exp[t/T_2 + \\ & i \int_0^t \omega_0(t') dt'] M_z \end{aligned} \quad (A6)$$

The second term on the right oscillates rapidly and should contribute to  $m_x$  an amount of the order of  $M_0 b_x B_0$  which we assume to be negligible for  $b_x \ll B_0$ . This term is thus dropped. Define  $q_x$  by

$$\begin{aligned} m_x(\vec{r}, t) &= \\ \exp[-i\gamma \int_0^t b_x(\vec{r}, t') dt'] q_x(\vec{r}, t) \end{aligned} \quad (A7)$$

Substituting Eq. A7 into Eq. A6 yields

$$\begin{aligned} \dot{q}_x(\vec{r}, t) &= D \left\{ \exp[i\gamma \int_0^t b_x(\vec{r}, t') dt'] \right. \\ & \left. \nabla^2 \exp[-i\gamma \int_0^t b_x(\vec{r}, t') dt'] \right\} q_x(\vec{r}, t) \end{aligned} \quad (A8)$$

It is now assumed that  $b_x(\vec{r}, t)$  contains only a linear gradient term and can thus be written as

$$b_x(\vec{r}, t) = \vec{G}(t) \cdot \vec{r} = \sum_j G_j(t) x_j \quad (A9)$$

so that

$$\begin{aligned} \dot{q}_x(\vec{r}, t) &= D \exp[i\gamma \sum_j x_j \int_0^t G_j(t') dt'] \nabla^2 \\ & \exp[-i\gamma \sum_j x_j \int_0^t G_j(t') dt'] q_x(\vec{r}, t) \end{aligned} \quad (A10)$$

where  $\nabla^2$  operates on  $\exp[\dots]$  and  $q_x(\vec{r}, t)$ . To show that  $q_x(\vec{r}, t)$  is independent of  $\vec{r}$  for the initial conditions considered, let  $\vec{R}$  be a constant vector such that  $\vec{r} = \vec{R} + \vec{q}$ . Substitute this into Eq. A10 and take advantage of the fact that  $\nabla^2 = \nabla_q^2$  so that terms containing  $\vec{G}(t) \cdot \vec{R}$  can be passed through the  $\nabla_q^2$  operator. Then one gets

$$\begin{aligned} \dot{q}_x(\vec{q} + \vec{R}, t) &= \\ D \exp[i\gamma \int_0^t \vec{G} \cdot \vec{q} dt'] \nabla_q^2 \exp \\ & [-i\gamma \int_0^t \vec{G} \cdot \vec{q} dt'] q_x(\vec{q} + \vec{R}, t) \end{aligned} \quad (A11)$$

Thus  $q_x(\vec{r} + \vec{R}, t)$  has the same equation of motion as  $q_x(\vec{r}, t)$ , and if  $q_x(\vec{r}, t)$  is independent of  $\vec{r}$  at any time (such as at  $t = 0$ ), it is independent of  $\vec{r}$  at all times. Dropping the spatial dependence of  $q_x(\vec{r}, t)$  on  $\vec{r}$  and operating with  $\nabla^2$  in Eq. A10 yields

$$\dot{q}_x(t) = -\gamma^2 D \left[ \sum_{j=1}^3 \left( \int_0^t G_j(t') dt' \right)^2 \right] q_x(t) \quad (A12)$$

Solving this equation yields

$$q_x(t) = \exp[-\gamma^2 D \sum_j \int_0^t \left( \int_0^{t'} G_j(t'') dt'' \right)^2 dt'] q_x(0) \quad (A13)$$

It time  $t = t_e$  is now chosen to be the time of the occurrence of an echo, then

$$\int_0^{t_e} \omega_0(t) dt = \int_0^{t_e} b_x(\vec{r}, t') dt' = \int_0^{t_e} G_x(t') dt' = 0 \quad (A14)$$

for  $j = 1, 2$  and  $3$ . Then

$$\begin{aligned} M_x(\vec{r}, t_e) &= \\ \exp[-t_e/T_2 - \gamma^2 D \sum_j \int_0^{t_e} K_j^2(t') dt'] M_x(0, 0) \end{aligned} \quad (A15)$$

where

$$K_j(t') = \int_0^{t'} G_j(t'') dt'' \quad (A16)$$

Finally, the observed signal  $A(t)$  is proportional to  $\int M_x(\vec{r}, t) dV$ , integrated over the sample. Since  $M_x(\vec{r}, t)$  is independent of  $\vec{r}$

$$A(t) = A_0(t) \exp[-\gamma^2 D \sum_j \int_0^{t_e} K_j^2(t') dt'] \quad (A17)$$

where

$$A_0(t) = \text{constant} \times \exp[-t/T_2] \quad (\text{A18})$$

### ACKNOWLEDGMENT

This work was supported by National Science Foundation Grant DMR 76-22655.

### REFERENCES

- <sup>1</sup> E.L. Hahn, *Phys. Rev.* **80**, 580 (1950).
- <sup>2</sup> H.Y. Carr and E.M. Purcell, *Phys. Rev.* **94**, 630 (1954).
- <sup>3</sup> E.O. Stejskal and J.E. Tanner, *J. Chem. Phys.* **42**, 288 (1965).
- <sup>4</sup> H.C. Torrey, *Phys. Rev.* **104**, 563 (1956).
- <sup>5</sup> R.F. Karlicek and I.J. Lowe, *J. Mag. Reson.* **37**, 75 (1980).
- <sup>6</sup> H.R. Prupacher, *J. Chem. Phys.* **56**, 101 (1972).
- <sup>7</sup> L.E. Drain, *Proc. Phys. Soc.* **80**, 1380 (1962).
- <sup>8</sup> R.F. Karlicek and I.J. Lowe, *Solid State Commun.* **31**, 163 (1979).